J. Astrophys. Astr. (2005) **26,** 171–184

# Excitation of Solar-like Oscillations: From PMS to MS Stellar Models

R. Samadi[1], M.-J. Goupil[1], E. Alecian[1], F. Baudin[2], D. Georgobiani[3], R. Trampedach[4], R. Stein[5] & Å. Nordlund[6]
[1]*Observatoire de Paris, 5 place J. Janssen, 92195 Meudon, France.*
[2]*Institut d'Astrophysique Spatiale, Orsay, France.*
[3]*Center for Turbulence Research, Stanford University NASA Ames Research Center, Moffett Field, USA.*
[4]*Research School of Astronomy and Astrophysics, Mt. Stromlo Observatory, Weston, Australia.*
[5]*Michigan State University, East Lansing, USA.*
[6]*Niels Bohr Institut, Copenhagen, Denmark.*

**Abstract.** The amplitude of solar-like oscillations results from a balance between excitation and damping. As in the sun, the excitation is attributed to turbulent motions that stochastically excite the $p$ modes in the uppermost part of the convective zone. We present here a model for the excitation mechanism. Comparisons between modeled amplitudes and helio and stellar seismic constraints are presented and the discrepancies discussed. Finally the possibility and the interest of detecting such stochastically excited modes in pre-main sequence stars are also discussed.

*Key words.* Turbulence—convection—oscillations—excitation—sun, stars: $\alpha$ Cen A—stars: main and pre-main sequence stars.

## 1. Introduction

In the past approximately five years, solar-like oscillations have been detected in several intermediate massive stars lying on the main sequence (e.g., Procyon, $\alpha$ Cen A and B, $\beta$ Hydri, $\beta$ Vir, HD 49933, etc.), in early post-main sequence stars (e.g., $\eta$ Boo) and also in red giant stars ($\xi$ Hya, $\epsilon$ Oph, $\eta$ Ser). We refer the reader to the recent review by Kjeldsen & Bedding (2004).

Those oscillations are stochastically excited by turbulent motions in the uppermost part of the convective zone. This mechanism has been modeled by several authors in different ways (e.g., Goldreich & Keeley 1977; Christensen-Dalsgaard & Frandsen 1983; Balmforth 1992; Goldreich *et al.* 1994; Samadi & Goupil 2001). Those approaches differ from each other by the nature of the assumed excitation sources, the assumed simplifications and approximations and also by the way turbulent convection is described (see the review by Stein *et al.* 2004).

Among the different theoretical approaches, that by Samadi & Goupil (2001, Paper I hereafter) includes a detailed treatment of the properties of turbulent convection. This formalism then offers the advantage of testing different assumptions about turbulent convection in stars. We briefly present this formalism in section 2 (see also the detailed summary by Samadi 2001). Section 3 explains how the mode excitation rates may be

computed – according to this formalism – from 1D stellar models or 3D simulation of stellar convection.

Provided that measurements of the oscillation amplitudes and life-times (or linewidths) are available it is possible to compute the rate $P$ at which energy is injected into the modes and hence to derive constraints on the models of stochastic excitation. The way those constraints are derived from seismic observations is summarized in section 4.

Such measurements have been available for the sun for several years (e.g., Chaplin *et al.* 1997, 1998; Libbrecht 1988). Based on the approach of Paper I and constraints from a 3D simulation of the sun, Samadi *et al.* (2003b, hereafter Paper IV) have found a rather good agreement between predicted excitation rates $P$ and excitation rates inferred from the helioseismic observations by Chaplin *et al.* (1998), except at high frequency where the discrepancy is substantial. However, recently, Baudin *et al.* (2005) have investigated in detail, the difficult problem of inferring solar $p$ mode excitation rates from the helioseismic data. Large differences between the new constraints obtained by Baudin *et al.* (2005) and those derived from Chaplin *et al.*'s (1998) are found. The computed excitation rates $P$ are found to be in even better agreement with the new constraints.

Recently Bedding *et al.* (2004) have derived – from recent seismic observations by Butler *et al.* (2004) – oscillation amplitudes and also averaged estimates of the oscillation life-times for $\alpha$ Cen A. Those data enable us to constrain $P$ for that star. The approach adopted in the case of the sun has thus been extended to the case of $\alpha$ Cen A and large discrepancies have been found for this star between predicted $P$ and "observed" $P$ (see Samadi *et al.* 2004).

For other stars, we may not yet derive observational constraints on $P$ but only on the mode amplitudes (mode linewidths are then taken from theoretical calculations). Theoretical calculations performed in the past approximately five years, resulted in an *overestimation* of the amplitudes of the solar-like oscillations detected in stars hotter and more massive than the sun such as $\eta$ Bootis, Procyon, $\xi$ Hydrae (see Kjelsen & Bedding 2001; Houdek & Gough 2002). This overestimation of the mode amplitudes may be attributed either to an overestimation of the excitation rates or an underestimation of the damping rates. In turn, any overestimation of the excitation rates may be attributed either to the excitation model *itself* or to the underlying convection model.

Numerical 3D simulations enable one to compute directly $P$ for stars with various temperatures and luminosities (see Nordlund & Stein 2001). Hence, using this method, Samadi *et al.* (2005a, Paper V) have computed, for seven 3D simulations of outer layers of main sequence stars – for which solar-like oscillations are expected – the rates at which energy is expected to be injected into $p$ modes. Comparison between these 3D calculations and those obtained using the theoretical model of stochastic excitation then provide a test of the validity of that theoretical model across the HR diagram. This test performed by Paper V is summarized in section 6.1.

Solar-like oscillations have so far been detected in main sequence stars as well as in red giant stars. However Samadi *et al.* (2002) predicted that one may also expect solar-like oscillations with large amplitudes in $\delta$ Scuti stars. As mentioned in that paper, there would be advantages in observing simultaneously opacity-driven and stochastically excited modes in the same $\delta$ Scuti star.

Pre-Main Sequence stars (PMS hereafter) are young objects on their way to the main sequence (MS hereafter). Prior to their arrival to the Zero Age Main Sequence

(ZAMS), their outer layers have the same properties as their MS counterpart in the HR diagram. For this reason, we expect stochastically excited modes in such objects. Detecting such oscillations would be a valuable way of probing the modeling of such active and very fast rotating young objects.

We have computed, for a representative set of Herbig Ae stars and T-Tauri stars, the rates at which energy is expected to be injected into the stable $p$ modes of such stars. The results of this new investigation are presented in section 6.2.

Computation of the amplitudes of solar-like oscillations in terms of Doppler velocity ($V$) requires – in addition to $P$ – the calculation of the mode damping rates $\eta$. Such calculations must be performed with a non-adiabatic pulsation code that takes into account not only the modulation of the radiative flux by the pulsation but also the interaction between pulsation and convection. Modeling this interaction is difficult. Several attempts have been made such as Gough's (1977) time-dependent model of convection, Gabriel's formalism (see e.g., Grigahcène *et al.* 2005) and Xiong's approach (see e.g., Xiong *et al.* 1998).

Using Gough's approach, Samadi *et al.* (2001b) have calculated $\eta$ – as in Houdek *et al.* (1999) – for a set of solar-like oscillating stars lying on the main sequence. Finally from that calculation and predicted values of $P$, we have computed $V_{\max}$, the maximum of $V$, across the main sequence for different assumptions (Paper V). It was found that, provided that the improved model of Paper IV is adopted, computed $V_{\max}$ are closer to the observed one than previous calculations. Section 7.1 presents this result.

Finally we extrapolate, in section 7.2, the calculations of $V_{\max}$ – obtained for main sequence stars – for pre-main sequence stars and we conclude whether or not solar-like oscillations may be detected in such stars with current or future instruments devoted to stellar seismology.

Section 8 is devoted to a discussion of the current status of modeling the excitation of solar-like oscillations.

## 2. The theoretical model of stochastic excitation

The theoretical model of stochastic excitation considered here is basically that of Paper I. In this model, two sources are associated with the driving of the resonant modes of the stellar cavity: the first one is related to the Reynolds stress tensor and as such represents a mechanical source of excitation. The second one is caused by the advection of the turbulent fluctuations of entropy by the turbulent motions (the so-called "entropy source term") and as such represents a thermal source of excitation.

The problem of the mode driving is solved in the framework of Goldreich & Keeley (1977)'s approach: the method consists of solving first the propagation of the *adiabatic* modes in the stellar cavity *without* the presence of turbulent convection. The solutions of this problem are the well-known adiabatic (real) displacement eigenvectors, that is: $\vec{\xi}(\vec{r}, t) = \vec{\xi}(\vec{r})e^{-i\omega_0 t}$ where $\omega_0$ is the oscillation eigenfrequency. We then add the turbulence and search the general solution for the mode velocity, $\vec{v}_{\rm osc}$, in the form:

$$\vec{v}_{\rm osc} = \frac{1}{2}(i\omega_0\, A(t)\, \vec{\xi}(\vec{r})\, e^{-i\omega_0 t} + cc), \tag{1}$$

where $cc$ means complex conjugate and $A(t)$ is an instantaneous amplitude that accounts for the driving by turbulent convection.

From the perturbed equation of continuity and motion and with the help of several simplifications, one derives a general expression for the mean square of $A$ (see details in Paper I):

$$\langle |A|^2 \rangle = \frac{1}{8\eta(\omega_0 I)^2} \left(C_R^2 + C_S^2\right), \tag{2}$$

where $\eta$ is the mode damping rate, $I \equiv \int_V \rho_0 \, d^3x \, (\vec{\xi}^* \cdot \vec{\xi})$ is the mode inertia, $C_R^2$ and $C_S^2$ are the turbulent Reynolds stress and entropy contributions respectively:

$$C_R^2 = \frac{64}{15}\pi^3 \int_0^M \mathrm{d}m \, \rho_0 \left(\frac{\mathrm{d}\xi_r}{\mathrm{d}r}\right)^2 \int_0^\infty \mathrm{d}k \int_{-\infty}^{\infty} \mathrm{d}\omega \, \frac{E^2(k)}{k^2} \chi_k(\omega_0 + \omega, r) \, \chi_k(\omega, r), \tag{3}$$

$$C_S^2 = \frac{16}{3}\frac{\pi^3}{\omega_0^2} \int d^3x_0 \, (\alpha_s g_r)^2 \, g_r \int \mathrm{d}k \int_{-\infty}^{+\infty} \mathrm{d}\omega \, \frac{E_s(k) E(k)}{k^2} \chi_k(\omega_0 + \omega) \chi_k(\omega). \tag{4}$$

In equation (3), $E(k)$ is the turbulent kinetic energy spectrum, $\chi_k(\omega)$ is the eddy time-correlation function in the frequency space, $\rho_0$ is the mean density. In equation (4), $E_s(k)$ is the turbulent spectrum of the entropy fluctuations, $g_r(\vec{\xi}_r, r)$ is a function that involves the first and the second derivatives of $\xi$ (see Samadi *et al.* (2003a, Paper III hereafter)) and finally $\alpha_s \equiv (\partial p/\partial s)_\rho$ where $p$ is the pressure and $s$ the entropy.

The time-averaged mode energy is given by

$$E = \int_0^M \mathrm{d}m \, \langle v_{\mathrm{osc}}^2 \rangle = \frac{1}{2} \, \langle |A|^2 \rangle \, I \omega_0{}^2, \tag{5}$$

where $\langle |A|^2 \rangle$ is the mean square amplitude as given by equation (2). The energy supply per unit time into each mode is given by (see Samadi *et al.* 2001, hereafter Paper II):

$$P \equiv \frac{d}{\mathrm{d}t} E = 2\eta \, E = \eta \, \langle |A|^2 \rangle \, I \, \omega_0^2. \tag{6}$$

The kinetic energy spectrum $E(k)$ is normalized as

$$\frac{1}{2} \, \langle u^2(\vec{x}_0) \rangle \equiv \int_0^\infty \mathrm{d}k \, E(k) = \frac{1}{2} \, \Phi w^2, \tag{7}$$

where $w$ is the rms of the vertical component of the velocity and $\Phi$ is a mean anisotropy factor introduced by Gough (1977) to take into account anisotropy effects at large scales (see equation (2) of Paper IV). The turbulent pressure is defined as usual as $p_t \equiv \rho_0 \, w^2$. Accordingly the driving by the Reynolds term is the largest where $p_t$ is the largest, that is generally at the top of the convective envelope.

As for $E(k)$, the entropy spectrum $E_s(k)$ is normalized as:

$$\frac{1}{2} \langle s_t^2(\vec{x}_0) \rangle = \int_0^\infty \mathrm{d}k \, E_s(k) = \frac{1}{2} \tilde{s}^2, \tag{8}$$

where $\tilde{s}$ is the rms of the entropy fluctuations. One shows that $\tilde{s}^2 = F_c^2/(\rho_0 T_0^2 p_t)$ where $F_c$ is the convective flux and $T_0$ the mean temperature (see Samadi *et al.* 2005b). Accordingly the driving by the so-called entropy source term is the largest where $F_c/(\rho_0 T_0)$ is the largest, that is at the top of the convective envelope where the density and temperature drop rapidly.

## 3. Methods for the calculation of the *p* mode excitation rates

The rate $P$ at which energy is injected per unit time into a mode is calculated according to the set of equations (6), (2), (3) and (4). The calculation thus requires the knowledge of quantities that are of three different types:

(1) Quantities that are related to the oscillation modes: the eigenfunctions ($\xi_r$) and associated eigenfrequencies ($\omega_0$).
(2) Quantities that are related to the spatial and time averaged properties of the medium: $\rho_0$, $\alpha_s$, $w$, $\tilde{s}$ and $\Phi$.
(3) Quantities that contain information about spatial and temporal correlations of the convective fluctuations: $E(k)$, $E_s(k)$ and $\chi_k(\omega)$.

Eigenfrequencies and eigenfunctions (in (1) above) are computed with an adiabatic pulsation model using a 1D stellar model. The spatial and time averaged quantities in (2) may be obtained either from a 3D simulation of the stellar surface or from a 1D stellar model. In the latter case, the calculation of $w$ and $\tilde{s}$ relies on the mixing-length formulation of convection and introduces free parameters (such as the mixing-length parameter and $\Phi$). Finally, for the quantities in (3), one may either obtain constraints from a 3D simulation or assume some models such as those investigated in Paper II. In the latter case, new adjustable parameters must generally be introduced as the scale length of the most energetic eddies and the parameter $\lambda$, which controls our lack of precise knowledge of the eddy time-correlations (see Paper IV).

The results presented here are based on different strategies and assumptions for the calculation of the quantities in (1), (2) and (3).

## 4. Inferring the mode excitation rates from seismic observations

The mode excitation rates may be inferred from the observations according to the relation:

$$P_{\rm obs}(\omega_0) = 2\,\pi\,\Gamma_\nu\,\mathcal{M}\,v_s^2(\omega_0), \tag{9}$$

where $\mathcal{M} \equiv I/\xi_{\rm r}^2(h)$ is the mode mass, $h$ the height above the photosphere where oscillations are measured, $\Gamma_\nu = \eta/\pi$ the mode linewidth at half maximum (in Hz) and $v_s$ the rms of the mode surface velocity.

As pointed out by Baudin *et al.* (2005), the layer ($h$) where the mode mass is evaluated must be properly estimated to derive correct values of the excitation rates. Indeed solar seismic observations in Doppler velocity are usually measured from a given spectral line. The layer where oscillations are measured then depends on the height where the line is formed. Different instruments use different solar lines and

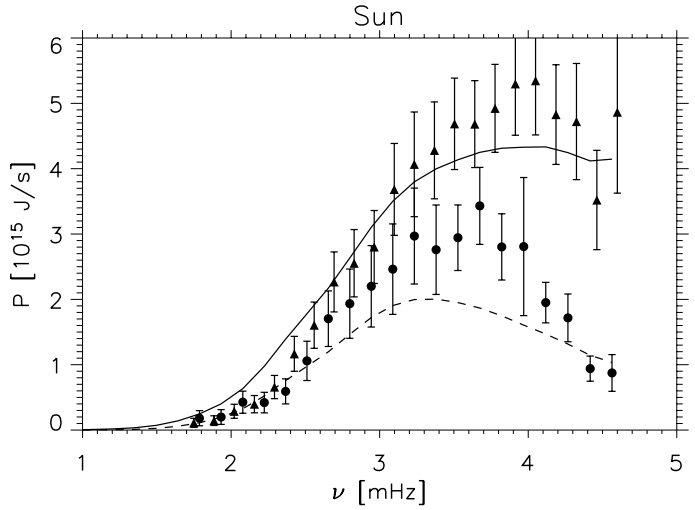


**Figure 1.** Rates $P$ at which energy is injected into the solar modes. Filled circles and triangles: excitation rates $P$ inferred from the observations according to equation (9). The circles correspond to seismic observations from the BiSON network as quoted by Chaplin *et al.* (1998) and the triangles to that from the GOLF instrument as quoted by Baudin *et al.* (2005). Continuous and dashed lines correspond to predicted excitation rates computed as explained in section 5. The continuous (dashed resp.) line corresponds to a calculation in which $\chi_k$ is assumed Lorentzian (Gaussian resp.).

then probe a different region of the atmosphere. The BiSON instruments use the KI line whose height of formation is estimated at the height $h \approx 280$ km while the GOLF instrument uses the Na I D1 and D2 lines whose height of formation is estimated at the height $h \approx 340$ km (see Baudin *et al.* 2005). In Fig. 1, $P_{\rm obs}$ are calculated with mode masses evaluated at $h = 280$ km for the BiSON data set reduced by Chaplin *et al.* (1998) and at $h = 340$ km for the GOLF data set reduced by Baudin *et al.* (2005).

## 5. *p* mode excitation in the sun

The rate $P$ at which energy is injected into solar $p$ modes, was computed in Paper III and IV as follows: the calculations of $\xi_r$ and $\omega_0$ were performed on the base of a 1D solar model built according to Gough's (1977) non-local formulation of the mixing-length theory (GMLT hereafter). Values of $\rho_0$ and $\alpha_s$ were also obtained from this 1D GMLT's model. On the other hand, the quantities $w$, $\tilde{s}$ and $\Phi$ – that are related to the averaged properties of turbulent convection – were calculated directly from a 3D simulation of the solar surface with a spatial mesh grid of $253 \times 253 \times 163$ (see details in Paper III and IV). Furthermore the analytical models adopted for $E(k)$ and $\chi_k$ were also constraints by the 3D simulation.

It was shown from the 3D simulation that a Gaussian – usually used for modeling $\chi_k$ – is inadequate (Paper IV): a Lorentzian fits best the frequency dependence of $\chi_k$.

As shown in Fig. 1 with the dashed line, the use of a Gaussian for $\chi_k$ underestimates $P_{\rm obs}$ while a Lorentzian results in values of $P$ closer to the different solar seismic constraints.

This result then shows that, provided that such a non-Gaussian model is assumed, the present model of stochastic excitation is – for the sun – rather satisfactory, without adjustment of free parameters.

Some discrepancies still exist between $P$ and $P_{\rm obs}$ as well as between the different seismic data analysis. In Fig. 1, $P$ obtained with a Lorentzian is closer to $P_{\rm obs}$ inferred from the seismic data reduction by Baudin *et al.* (2005) whereas large discrepancies are obtained at high frequency with the values of $P_{\rm obs}$ inferred from Chaplin *et al.*'s (1998) data set. Furthermore we find that the height where $\mathcal{N}$ in equation (9) is evaluated changes $P_{\rm obs}$ significantly (not shown). We then conclude that inferring excitation rates from the seismic observations remains difficult and provides constraints on $P$ with still important uncertainties.

## 6. *p* mode excitation across the HR diagram

### 6.1 *Main sequence stars*

We consider a set of 3D simulations of solar-like oscillating stars. We compute internal structure of 1D stellar models and associated eigenfunctions consistent with the 3D simulations. We then compute, on the basis of the current theoretical model of stochastic excitation, the rates at which energy is expected to be injected into the modes. The calculation is performed as explained in Samadi *et al.* (2005a) and as summarized below: the calculation of $\xi_r$ and $\omega_0$ is performed using a 1D stellar model consistent with the simulations of stars. The total kinetic energy contained in the turbulent kinetic spectrum, $E(k)$, its depth dependence, and its $k$-dependence are obtained directly from the 3D simulation. For the eddy time-correlation function $\chi_k$, we investigate both a Gaussian and a Lorentzian. Results are shown in Fig. 2 (left).

As mentioned in the introduction, the energy injected into the mode may be directly calculated from a 3D simulation of the outer layer of the star. This calculation has been done for the sun by Stein & Nordlund (2001) according to the expression proposed by Nordlund & Stein (2001) (their equation (74)), which corresponds to the direct calculation of $pdV$ work of the non-adiabatic gas and turbulent pressure (entropy and Reynolds stress) fluctuations on the modes. This method has been applied in Paper V to seven 3D simulations of the outer layers of main sequence stars. The result of this calculation is presented in Fig. 2 (left) by the triangles labeled as $P_{\rm 3D}$. These calculations are then compared with those obtained on the basis of the theoretical model of stochastic excitation.

A rather good agreement is found between $P_{\rm 3D}$ and the calculations in which a Gaussian or an exponential (not shown) is assumed while a Lorentzian results in $P$ much larger than $P_{\rm 3D}$.

In contrast to what was found in the case of the solar 3D simulation investigated in Paper IV (see section 5), the inferred $\nu$ dependencies of $\chi_k$ are far from a Lorentzian. This discrepancy is explained by the fact that the simulations investigated in Paper V have all a too small resolution compared to that considered in Paper IV. However, by investigating solar simulations with different resolutions, we find that, as the spatial resolution increases, $\chi_k$ tends towards a Lorentzian $\nu$-dependence.

We find that $P_{\rm max}$ scales as $(L/M)^s$ where $s$ is the slope of the scaling law, $L$ is the luminosity and $M$ is the mass of the 1D models associated with the 3D simulations. This result is not surprising: indeed, even though the ratio $L/M$ is the ratio of two

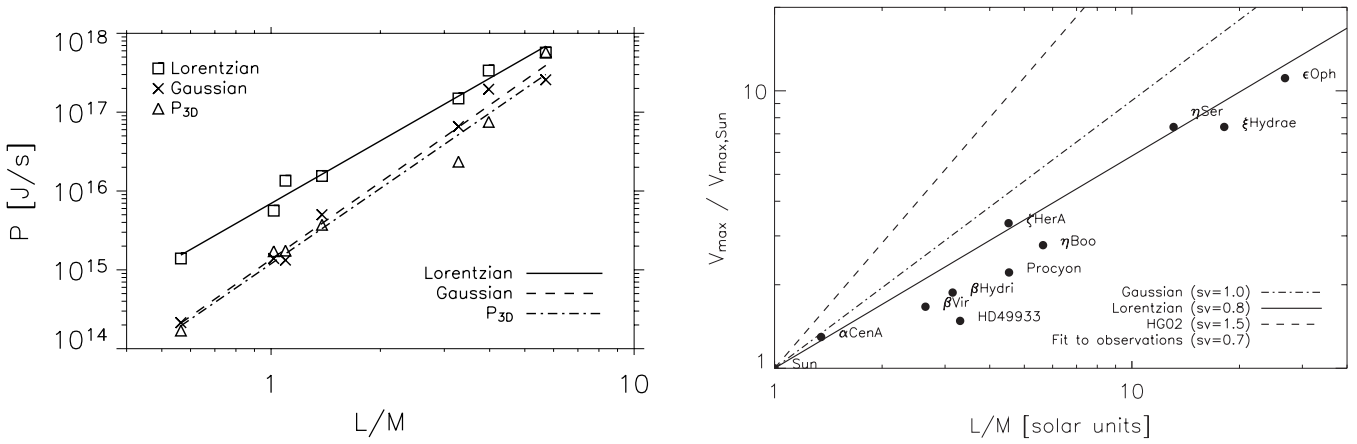


**Figure 2.** **Left:** $P_{\max}$ versus $L/M$ where $L$ is the luminosity and $M$ is the mass of the 1D models associated with the 3D simulations. The triangles correspond to the direct calculations (labeled here as $P_{3D}$) and the other symbols correspond to calculations based on the theoretical model of stochastic excitation and using the two forms of $\chi_k$: the crosses assume a Gaussian and the squares a Lorentzian, respectively. The lines are the results of fitting each set of symbols with a power law of the form $(L/M)^s$ where $s$ is the slope of the power law. **Right:** Same as left panel for $V_{\max}/V_{\max,\odot}$, the maximum of the mode amplitudes relative to the observed solar value ($V_{\max,\odot} = 27\,\mathrm{cm\,s^{-1}}$). The filled circles correspond to the few stars for which solar-like oscillations have been detected in Doppler velocity. The solid and the dot dashed lines are the result of fitting the calculations performed with a Lorentzian and a Gaussian, respectively, with a power law of the form $(L/M)^{sv}$ where $sv$ is the slope of the power law (see section 7.1). The dot dot dashed line is the result of fitting the observations with such power law. For comparison the dashed line shows the power law obtained by Houdek & Gough (2002).

global stellar quantities, it nevertheless characterizes essentially the stellar surface layers where the mode excitation is located since $L/M \propto T_{\rm eff}^4/g$.

The value found for $s$ is sensitive to the choice for $\chi_k$: indeed the Gaussian results in $s = 3.3$ and the Lorentzian in $s = 2.6$. Seismic observations in the sun (see section 5) and in $\alpha$ Cen A tend to favor the Lorentzian over the Gaussian. For other stars for which stochastically excited $p$ modes are expected, the Lorentzian is likely to remain the best form for $\chi_k$ (see section 7.1), but this needs to be confirmed with data providing constraints on the excitation rates $P$. The high-quality data of the COROT instrument will enable us to derive $P_{\rm max}$ as a function of $L$ and $M$ for the different target stars. These data will very likely enable us to determine the appropriate model for the eddy time-correlations ($\chi_k$).

### 6.2 *Pre-main sequence stars*

$p$ mode excitation has so far been studied in main sequence stars. We consider here a set of 1D models of pre-main sequence stars (PMS).

Our evolutionary models are computed with the CESAM code written by Morel (1997). The assumed physics is standard and very similar to that described in Lochard *et al.* (2005): the external boundary condition is defined in a simplified model atmosphere involving the Eddington $T(\tau)$ law. The adopted mean chemical composition for the sun is taken as $X_0 = 0.715$, $Y_0 = 0.267$, and $Z_0 = 0.018$. The convective flux is computed according to the classical prescription of the Mixing Length Theory (Böhm-Vitense (1958)). The mixing length value $l_{\rm MLT}$ is equal to 1.62 $H_P$. No diffusion and no rotation are included in stellar model computations.

We have computed nine models of PMS stars with masses ranging from $M = 1\,{\rm M}_\odot$ to $M = 1.8\,{\rm M}_\odot$. Their locations in the HR diagram are shown in Fig. 3 (left). They are labeled from 1 to 9. The evolutionary tracks associated with those computed PMS models are also presented. The evolution of a PMS star may be decomposed into two different phases. The first phase corresponds to a fast contraction. During this phase the contraction time scale is of the same order as the dynamic time scale. The second phase, on the other hand, is characterized by a contraction time scale longer than the dynamic time scale. During this phase the usual quasi-static approximation then holds (see Suran *et al.* 2001) and the models computed by CESAM may be considered representative (except effects of fast rotation that are not included here).

Most of the models are chosen at a late stage of the second phase, before the stars reach the MS except model number 3 that is located at the beginning of the second phase.

Among our set of models, two of them (models 8 and 9) have $M \gtrsim 1.7\,{\rm M}_\odot$and are thus representative of Herbig Ae stars. Furthermore both lie on the instability strip predicted by Dupret *et al.* (2004). All other models have a mass $M \lesssim 1.7\,{\rm M}_\odot$ and thus correspond to T-Tauri stars.

We next compute $P_{\rm max}$ for each model as follows: as for the other case (sections 5 and 6.1), the calculation of $\xi_r$ and $\omega_0$ is based on the 1D model and makes use of an adiabatic pulsation code. However the input quantities related to the spatial and time averages of the medium are obtained from the 1D models, which rely on the classical mixing-length. For the $k$-dependency of the kinetic energy spectrum, $E$, we assume as in Paper III and IV, the spectrum that fits best the spectrum obtained in the solar 3D simulation investigated in those papers. Finally we adopt a Lorentzian for $\chi_k$.

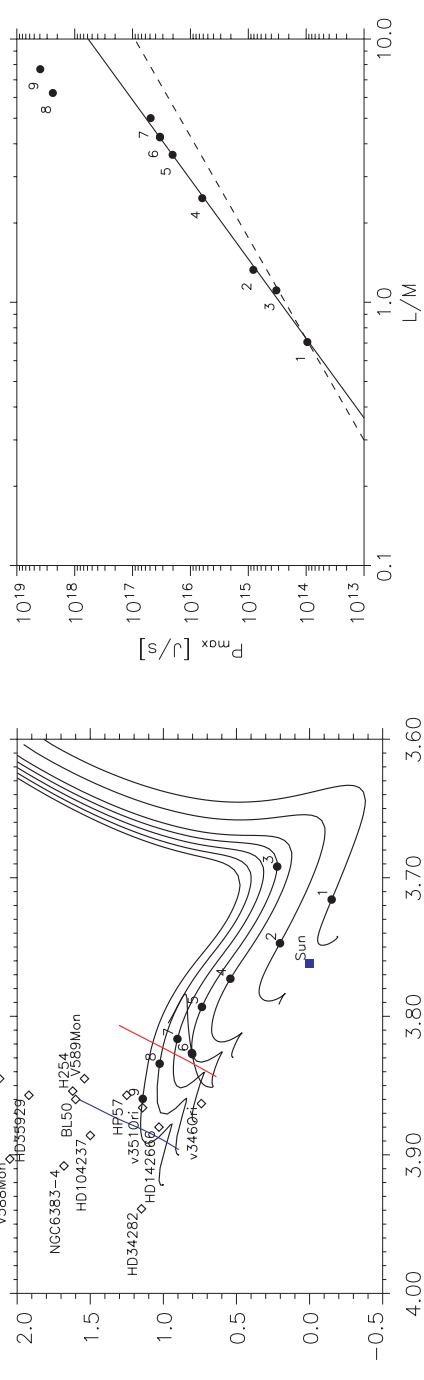


**Figure 3.** **Left:** Location of PMS stars on the HR diagram. The diamonds correspond to the PMS stars for which unstable modes have been detected (according to Table 2 of Marconi & Palla 2003). The filled circles with associated numbers correspond to computed PMS models with different ages and masses. The diagonal lines correspond to the red and blue edges of the instability strip as predicted by Dupret *et al.* (2004) for the radial modes. The evolutionary tracks of PMS models with masses ranging from $M = 1\,M_{\odot}$ to $M = 1.8\,M_{\odot}$ are also represented. **Right:** The filled circles correspond to the maximum of mode excitation rates obtained as explained in section 6.2 for the PMS models shown in the left panel. The continuous line is the result of fitting the set of dots with a power law of the form $(L/M)^s$ where $s$ is the slope of the power law (models with number 8 and 9 have been discarded from the fit, see text). The dashed line corresponds to the power law $(L/M)^{2.6}$ obtained with calculations performed on the base of 3D simulation constraints and assuming a Lorentzian for $\chi_k$ (see section 6.1).

The results of the calculation of $P_{\max}$ are shown in Fig. 3 (right). Except for models 8 and 9, $P_{\max}$ may be nicely fitted with a power law of the form $(L/M)^s$ with $s = 3.3$. Hence, as for the main sequence stars, $P_{\max}$ increases with the ratio $L/M$ according to a power law. This result is not surprising. Indeed, as for MS stars, $p$ mode excitation occurs at the surface of the star that is characterized by a given $T_{\rm eff}$ and a given $g$ (we recall that $L/M \propto T_{\rm eff}^4/g$ ).

This slope of the power law is however somewhat larger than the one found with the set of main-sequence stars investigated in section 6.1. The difference is likely to be connected with the fact that the calculations in section 6.1 used constraints from the 3D simulations whereas those performed here rely on the mixing-length theory. However the physical reasons are not yet identified.

Models 8 and 9 result in larger $P_{\max}$ than one would except with the fitted power law. In contrast with the other models, those two models have two separated super-adiabatic layers. The mode driving hence occurs within two different regions and is thus stronger than if those stars had only one super-adiabatic layer.

## 7. *p* mode amplitudes across the HR diagram

Calculation of the rms value of the mode surface velocity, $v_s$, requires the knowledge of the mode excitation rate ($P$) and the mode damping rate ($\eta$). Indeed according to equation (9), $v_s^2$ is related to $P$ and $\eta$ as:

$$v_s^2 = \frac{1}{\mathcal{M}} \frac{P}{\eta}, \tag{10}$$

where $\mathcal{M}$ is the mode mass evaluated at the photosphere (*i.e.*, at $r = R_{\rm eff}$).

### 7.1 *Main sequence stars*

In Samadi *et al.* (2001b), calculations of the damping rates $\eta$ based on Gough's time-dependent and non-local treatment of convection were performed for different stellar models with different values of $L$ and $M$. On the other hand, as summarized in sections 6.1 and 6.2, $P_{\max}$ scales as $(L/M)^s$ where the slope $s$ depends on the choice for $\chi_k$. Then, according to equation (10), we may determine $V_{\max}(L, M)$ for the different power laws of $P_{\max}$. Each set of calculations is next fitted by a power law of the form $(L/M)^{sv}$. This was done in Paper V and the result is shown in Fig. 2 (right).

As for $P_{\max}$, the slope of the power law for $V_{\max}(L, M)$ depends on the assumptions for $\chi_k$, that is $sv = 1.0$ when $\chi_k$ is Gaussian and $sv = 0.8$ when it is Lorentzian.

Solar-like oscillations have been detected in Doppler velocity in about $\sim 10$ stars. The maximum amplitudes of those oscillations are represented in Fig. 2 (right) with the filled circles. As already stressed by Kjeldsen & Bedding (1995), the amplitudes clearly scale approximately as $(L/M)^{sv}$.

"The observed dependence of $v_{\max}$ on the ratio $L/M$ may be qualitatively explained as follows: As already noticed in Sect. 6.1, the maximum of the excitation rate, $P_{\max}$, scales as $(L/M)^s$. We recall that $L/M \propto T_{\rm eff}^4/g$. The p mode excitation occurs at the surface of the star that is characterized by a given $T_{\rm eff}$ and a given $g$. Hence the larger $T_{\rm eff}$, the larger the convective flux. Moreover the smaller $g$ or the larger $T_{\rm eff}$, the larger the pressure scale height and hence the larger the eddy size (see also

Kjeldsen & Bedding 1995). Now, the larger the eddy size or the larger the convective flux, the larger the excitation (c.f. Eq. 65 of Paper I)".

A fit to the observations results in $sv \simeq 0.7$. As seen in Fig. 2 (right) calculations based on a Lorentzian for $\chi_k$ result in power law closer to that derived from the observations than those based on Gaussian. As a conclusion, as in the sun (see section 5) and in $\alpha$ Cen A, the observations tend to confirm that the Lorentzian is an approximately correct form for $\chi_k$.

For comparison with previous results, the dashed line in Fig. 2 (right) shows the power law proposed by Houdek & Gough (2002). This power law clearly overestimates by a large amount the oscillation amplitudes observed in the stars more luminous than the sun. From this result, we conclude that the problem of the overestimation of the amplitudes of the solar-like oscillating stars more luminous than the sun is directly related to the choice of the model for $\chi_k$.

### 7.2 *Pre-main sequence stars*

To compute the mode amplitudes associated with our PMS models we must in principle compute the mode damping rates. However for the high frequency $p$ modes, the mode damping occurs mainly at the stellar surface. So we may expect that modes are damped at the same level as for the MS stars because MS and PMS stars have similar envelope properties. We may then expect that the mode amplitudes will vary as for the MS stars as $(L/M)^{sv}$, with a similar slope $sv$ as found in section 7.1 (namely $sv = 0.7$).

Accordingly, $V_{\max}$ is expected to range between $\sim 20$ cm/s and $\sim 120$ cm/s for our set of stellar PMS models. To derive the mode amplitudes in terms of luminosity fluctuations, $(\mathrm{d}L/L)_{\max}$, we may – as in Lochard *et al.* (2005) – apply a crude conversion based on the adiabatic approximations (see Kjeldsen & Bedding 1995). This puts $(\mathrm{d}L/L)_{\max}$ in the range between $\sim 2$ ppm and $\sim 15$ ppm.

HARPS is currently among the best ground-based instruments devoted to the detection of solar-like oscillations. Indeed this instrument is able to detect solar-like oscillations in stars brighter than $m_v \sim 5$ (see e.g., Mosser *et al.* 2005). Unfortunately PMS stars are in general faint objects. For instance, the brightest known object has an apparent magnitude $m_v \sim 9$ (Marconi & Palla 2003). HARPS performances are still then too low to detect solar-like oscillations in the known PMS stars.

The CoRoT mission (see Baglin 2003) will be able to detect stochastically excited modes as low as in the sun (that is $(\mathrm{d}L/L)_{\max} \simeq 4$ ppm), or in stars of apparent magnitude around $m_v \sim 6$ and with a signal-to-noise ratio $(S/B)$ in the *power spectrum* better than 15. The instrument will be limited by the photon noise up to $m_v \sim 9$. For a star with magnitude $m_v \sim 8$, the (white) noise level will be of order 1.8 ppm, which will allow the detection of amplitudes larger than $\sim 7$ ppm with $S/B \gtrsim 15$.Above $m_v \sim 9$, the noise level is expected to increase very rapidly at a level difficult to predict now. Hence, the detection of solar-like oscillations in PMS stars is not guaranteed with the CoRoT instrument. On the other hand, a space based instrument with performances similar to that of the Eddington instrument (see Favata *et al.* 2000) will be able to detect solar-like oscillations in stars as faint as most of the known PMS stars.

## 8. Discussion

Although the current model of stochastic excitation results in excitation rates in good agreement with the values inferred from the solar seismic observations, there are still

important discrepancies with those derived from the recent seismic observations of $\alpha$ Cen A. In all cases the observations favor a Lorentzian for the eddy time-correlation function $\chi_k$ rather than a Gaussian. It is not yet clear whether the remaining discrepancies between the observations and the theory are related to the way the constraints are inferred from the observations or the assumptions and the simplifications adopted in the current theory.

Among the different simplifications involved in the theory, we believe that two of them are the most significant: First the model presented here is based on the strong assumption that the excitation is spatially isotropic (the medium anisotropy is only taken into account in average). Second, the calculation is based on the adiabatic (real) mode eigenvectors. Non-adiabatic effects are important in the region where the excitation occurs. They are expected to change the behavior of the eigenvectors in that region (work in progress).

## Acknowledgements

RS and MJG acknowledge support by Programme National de Physique Stellaire (PNPS, France) and by the Aryabhatta Research Institute of Observational Sciences (ARIES, Nainital, India). We thank C. Catala for fruitful discussions and Y. Lebreton for valuable help in building the PMS models.

## References

Baglin, A. 2003, *Advances in Space Research*, **131(2)**, 345.
Balmforth, N. J. 1992, *MNRAS*, **255**, 639.
Baudin, F., Samadi, R., Goupil, M. *et al.* 2005, *A&A*, **433**, 349.
Bedding, T. R., Kjeldsen, H., Butler, R. P. *et al.* 2004, *ApJ*, **614**, 380.
Böhm-Vitense, E. 1958, *Zeitschr. Astrophys*, **46**, 108.
Butler, R. P., Bedding, T. R., Kjeldsen, H. *et al.* 2004, *ApJ*, **600**, L75.
Chaplin, W. J., Elsworth, Y., Isaak, G. R. *et al.* 1997, *MNRAS*, **288**, 623.
Chaplin, W. J., Elsworth, Y., Isaak, G. R. *et al.* 1998, *MNRAS*, **298**, L7.
Christensen-Dalsgaard, J., Frandsen, S. 1983, *Solar Physics*, **82**, 469.
Dupret, M.-A., Grigahcène, A., Garrido, R., Gabriel, M., Scuflaire, R. 2004, *A&A*, **414**, L17.
Favata, F., Roxburgh, I., Christensen-Dalsgaard, J. 2000, In *The Third MONS Workshop*: *Science Preparation and Target Selection*, p. 49–54.
Goldreich, P., Keeley, D. A. 1977, *ApJ*, **212**, 243.
Goldreich, P., Murray, N., Kumar, P. 1994, *ApJ*, **424**, 466.
Gough, D. O. 1977, *ApJ*, **214**, 196.
Grigahcène, A., Dupret, M.-A., Gabriel, M., Garrido, R., Scuflaire, R. 2005, *A&A* (in press).
Houdek, G., Balmforth, N. J., Christensen-Dalsgaard, J., Gough, D. O. 1999, *A&A*, **351**, 582.
Houdek, G., Gough, D. O. 2002, *MNRAS*, **336**, L65.
Kjeldsen, H., Bedding, T. R. 1995, *A&A*, **293**, 87.
Kjeldsen, H., Bedding, T. R. 2001, In: *Proceedings of the SOHO 10/GONG 2000 Workshop: "Helio- and Asteroseismology at the dawn of the millennium"*, Vol. ESA SP-464, 361.
Kjeldsen, H., Bedding, T. R. 2004, In: *Proceedings of the SOHO 14/GONG 2004 Workshop: "Helio- and Asteroseismology: Towards a Golden Future"*, Vol. ESA SP-559, 101.
Libbrecht, K. G. 1988, *ApJ*, **334**, 510.
Lochard, J., Samadi, R., Goupil, M.-J. 2005, *A&A* (in press).
Marconi, M., Palla, F. 2003, *AP&SS*, **284**, 245.
Morel, P. 1997, *A&AS*, **124**, 597.
Mosser, B., Bouchy, F., Catala, C. *et al.* 2005, *A&A*, **431**, L13.
Nordlund, Å., Stein, R. F. 2001, *ApJ*, **546**, 576.

Samadi, R. 2001, In *SF2A-2001: Semaine de l'Astrophysique Francaise, E148* (astro-ph/0108363).
Samadi, R., Goupil, M. 2001, *A&A*, **370**, 136 (Paper I).
Samadi, R., Goupil, M., Lebreton, Y. 2001a, *A&A*, **370**, 147 (Paper II).
Samadi, R., Houdek, G., Goupil, M.-J., Lebreton, Y., Baglin, A. 2001b, In: *1st Eddington Workshop: Stellar Structure and Habitable Planet Finding*, Vol. ESA SP-485 (astro-ph/0109174), 87–94.
Samadi, R., Goupil, M.-J., Houdek, G. 2002, *A&A*, **395**, 563.
Samadi, R., Nordlund, Å., Stein, R. F., Goupil, M. J., Roxburgh, I. 2003a, *A&A*, **403**, 303. (Paper III).
Samadi, R., Nordlund, Å., Stein, R. F., Goupil, M. J., Roxburgh, I. 2003b, *A&A*, **404**, 1129 (Paper IV).
Samadi, R., Goupil, M. J., Baudin, F. *et al.* 2004, In: *Proceedings of the SOHO 14/GONG 2004 Workshop: "Helio- and Asteroseismology: Towards a Golden Future"*, Vol. ESA SP-559, 615.
Samadi, R., Georgobiani, D., Trampedach, R. *et al.* 2005a, submitted to A&A (Paper V).
Samadi, R., Kupka, F., Goupil, M.-J., Lebreton, Y., van't Veer-Menneret, C. 2005b, submitted to A&A.
Stein, R., Georgobiani, D., Trampedach, R., Ludwig, H.-G., Nordlund, Å. 2004, *Solar Physics*, **220**, 229.
Stein, R. F., Nordlund, Å. 2001, *ApJ*, **546**, 585.
Suran, M., Goupil, M., Baglin, A., Lebreton, Y., Catala, C. 2001, *A&A*, **372**, 233.
Xiong, D. R., Deng, L., Cheng, Q. L. 1998, *ApJ*, **499**, 355.